56th LPSC (2025) 1987.pdf

Plasma-atmosphere interactions and dynamics of carbon in laser-induced plasma: insights from laboratory study for carbonate characterization with LIBS on Mars. E. Clavé<sup>1</sup>, F. Seel<sup>1</sup>, K. Rammelkamp<sup>1</sup>, S. Schröder<sup>1</sup>, C. H. Egerland<sup>1</sup>, A. Lomashvili<sup>1</sup>, P. Hansen<sup>1</sup>, <sup>1</sup>DLR Institute for Optical Sensor System, Berlin (elise.clave@dlr.de).

**Introduction:** Laser-induced breakdown spectroscopy (LIBS) enables the fast and remote characterization of samples, without preparation, in a variety of environments. It relies on the laser ablation of a sample, which generates a plasma, which contains the chemical elements from the sample, in an excited state. The ablation plasma is a complex, dynamic object which absorbs laser light, expands in the surrounding medium (atmosphere), cools down and decays. Analysis of the intensity of emission lines in the LIBS spectrum enables both qualitative and quantitative assessment of the chemical composition of the analyzed target [1-4], but it requires some understanding of the influence of atmospheric conditions on the plasma emissions. Both the pressure and the composition of the atmosphere affect plasma emissions through processes like plasma confinement, energy loss and contribution of chemical species from the atmosphere [5-8].

Due to its many advantages, LIBS has been successfully used in space exploration. Three LIBS instruments have been deployed on Mars so far: ChemCam onboard NASA's Curiosity rover (2012-ongoing) [9-10], SuperCam onboard NASA's Perseverance rover (2021-ongoing) [11-12], MarsCode onboard the Chinese Zhurong rover (2021-2022) [13].

One challenge with LIBS on Mars is to characterize the carbon-content of a sample, since the Martian atmosphere (6 mbar of CO<sub>2</sub>) contributes some C and O signal in all LIBS spectra [7, 14-18].

**Objectives**: Our short-term objective is to characterize the plasma-atmosphere interactions and how they affect the carbon emissions. Longer-term, this should enable us to characterize and correct for the atmospheric contribution to the carbon emissions in LIBS in Martian atmospheric conditions.

**Method**: We use time-resolved LIBS and plasma imaging to study the dynamics of carbon in the plasma depending on the origin of the carbon: either the sample or the atmosphere.

The protocol: We observe the C I 248 nm emission for i) a graphite sample in 6 mbar of air (C-rich sample in C-free atmosphere\*); ii) an anhydrous Mg-sulfate sample in 6 mbar of CO<sub>2</sub> (C-free sample in C-rich atmosphere). Both samples are pellets from powders, pressed during 10 minutes under 5t. \*Although air is not actually C free, the contribution of carbon from air is negligible in this case.

*The setup:* We use a plasma imaging setup at DLR described in [19]. This setup enables time-resolved

LIBS analyses in controlled atmospheric conditions, but also to image the laser-induced plasma throughout its development and evolution, either using all plasma emissions or a specific line of interest.

Data acquisition: Two kinds of data were acquired: i) spectral data in the 240-255 nm range; ii) images of the C I 248 nm emission in the ablation plasma. In both cases, we acquired time series with delays between 100 ns and  $\sim 2 \mu s$ , with a gate of 100 ns; the signal from 10 laser shots was accumulated for each spectrum.

*Processing of spectral data*: The intensity of the C I 248 nm line is extracted by fitting the line with a baseline and Pseudo-Voigt profile.

Processing of images: As in previous plasma imaging studies, the three main steps of processing of plasma images are: i) cropping the image to exclude potential signal from other lines, and folding the image on its symmetry axis (half image is the mean of both sides) ii) denoising: we use a combination of Savitzky-Golay filter (size 21, order 3) and wavelet transform (db4, order 5); iii) apply an Abel inversion to account for the integration of signal along the line of sight (see [19] for details). The image processing pipeline is still being improved on, we present preliminary products.

## Results & Discussion:

Time resolved LIBS: Comparing the intensity and decay of the C I 248 nm line observed in our two experimental configurations (Fig. 1) showed that this line is more intense in sulfate/CO<sub>2</sub> than in graphite/air (over the first 1.5 µs at least, Fig 1c). This shows how significant atmospheric contributions are in LIBS spectra, and that the C content of the sample is likely only a 2<sup>nd</sup>-order contributor to the C I signal in Martian atmospheric conditions. Moreover, the decay curves reveal different temporal evolutions of this signal (Fig. 1d): the decay is monotonous in CO<sub>2</sub>, whereas in air, the signal increases during the first ~1 us before decaying. This is likely due to de-excitation of C II to C I during the first microsecond of plasma lifetime after ablation of graphite in air. This could indicate that the ratio of C II and C I populations in the sulfate/CO<sub>2</sub> configuration is lower than in graphite/air. In general, this would indicate lower plasma temperature, but in this case, it could be interpreted in two, not mutually exclusive ways. i) C contributes to the plasma from the very beginning of its lifetime in the graphite/air configuration, thus including the hottest conditions; on the other end, by the time atmospheric CO<sub>2</sub> is broken down and C can contribute to plasma emission in the 56th LPSC (2025) 1987.pdf

sulfate/CO<sub>2</sub> configuration, the plasma is already relatively colder. ii) Alternatively, the carbon could be concentrated in some colder region of the plasma in the sulfate/CO<sub>2</sub> configuration, resulting in this apparent lower contribution of C II compared to C I.

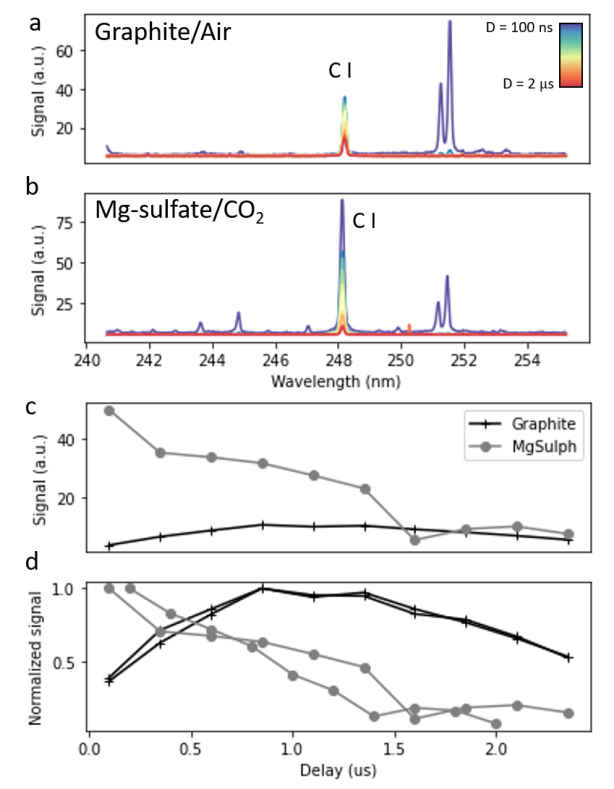


Fig. 1: Time-resolved spectra (a-b) and decay of C I signal (c-d) from graphite in 6 mbar of air and Mg-sulfate in 6 mbar of CO<sub>2</sub>. (d) shows two times series per configuration, with slightly different time parameters to show repeatability, normalized to the maximum signal per series.

Plasma imaging: Preliminary observations of the C I emission with plasma imaging show interesting differences between our two experimental configurations (Fig. 2). The C I emission covers a larger area in sulfate/CO<sub>2</sub> than in graphite/air. We would need to image all plasma emissions (as in [8]) to compare plasma sizes and determine if this reflects different plasma sizes in these two configurations, or if it shows different distributions of the C I emitters within the

emission plasmas. We also observe a rarefaction of C I emission at the center of the sulfate/CO<sub>2</sub> plasma, especially for delays of 700 ns and above, which is consistent with previous observations of the C I 248 nm line in gypsum in 6 mbar of CO<sub>2</sub> [19]. This is not observed in graphite/air, indicating different distributions of C I within these two plasmas, more in the central part in graphite/air and in an outer layer in sulfate/CO<sub>2</sub>.

Conclusions & Perspectives: We use time-resolved LIBS and plasma imaging to study plasma-atmosphere interactions, and in particular the dynamics of carbon in the ablation plasma depending on its origin: from the sample or from the atmosphere. We observe different temporal and spatial behaviors of C I in two experimental configurations where carbon comes exclusively from the sample (graphite in 6 mbar of air) or exclusively from the atmosphere (Mg-sulfate in 6 mbar of CO<sub>2</sub>). We highlight the significance of atmospheric contribution, generating a more intense C I emission than the carbonate contained in the graphite pellet.

The results in this abstract are preliminary, the study is ongoing and will include imaging the total emission as well as different emission lines, especially C II emission. Characterizing the dynamics of different ionization states of carbon depending on its origin should enable us to improve on the strategies for carbonate characterization with LIBS in Martian atmospheric conditions (choice of line, normalization, etc.).

References: [1] El Haddad, et al., SAB 2014; [2] Clegg et al., SAB 2016; [3] Anderson et al., SAB 2021; [4] Chen et al., SAB 2022; [5] Iida SAB 1990; [6] Knight et al., AS 2000; [7] Schröder et al., Icarus 2019; [8] Seel et al., Icarus 2024; [9] Maurice et al., SSR 2012; [10] Wiens et al., SSR 2012; [11] Maurice et al., SSR 2021; [12] Wiens et al., SSR 2021; [13] Xu et al., SSR 2021; [14] Gasnault et al., 2012; [15] Beck et al., LPSC 2016; [16] Beck et al., LPSC 2017; [17] Clavé et al., JGRP 2023; [18] Beck et al., SAB 2024; [19] Vogt et al., SAB 2021.

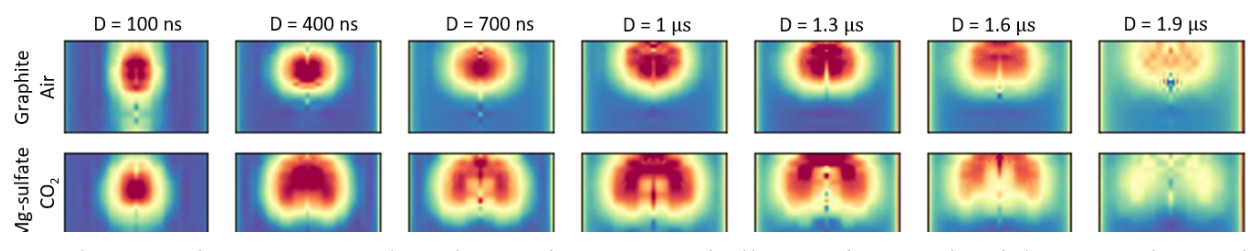


Fig. 2: Imaging the C I emission in plasma from graphite/air (top) and sulfate/CO<sub>2</sub> (bottom); after Abel inversion. The central axis presents processing artifacts, to be corrected.